Contribution from Los Alamos Scientific Laboratory, University of California, Los Alamos, New Mexico 87545, and the Department of Chemistry, University of Texas, Austin, Texas 78712

^{15}N Magnetic Resonance of Aqueous Imidazole and Zinc(II)–Imidazole Complexes. Evidence for Hexacoordination

MOHAMMED ALEI, JR.,*[1a] LEON O. MORGAN,[1b] and WILLIAM E. WAGEMAN[1a]

Received December 29, 1977

^{15}N NMR chemical shifts of doubly labeled [^{15}N]imidazole permit evaluation of hydrogen bonding, proton association, and Zn(II) complex formation in homogeneous solution. The ^{15}N resonant frequency in aqueous solutions of imidazole at pH 9–12 is independent of imidazole concentration, suggesting insignificant self-association via hydrogen bonding involving the N_3 lone pair and the N_1 proton of a neighboring molecule. Protonation at N_3 (pH <5) produces a 31.2-ppm diamagnetic shift and deprotonation at N_1 (pH >13) an ~20-ppm paramagnetic shift relative to neutral aqueous imidazole. Those shifts are very large compared to the ~±0.5-ppm uncertainty in the ^{15}N shift measurements. In solutions of Zn^{2+} and imidazole the ^{15}N resonance in $ZnIm_i^{2+}$ complexes (Im = imidazole) is diamagnetically shifted by 10–20 ppm relative to neutral aqueous imidazole. Over a range of ratios of total imidazole to total zinc such that the average number of complexed imidazole molecules per Zn^{2+} ($\bar{p}$) is ~3.5, or less, the shift data are well interpreted by a four-species model (i = 1–4) using stepwise formation constants from the literature. Significant deviations from that model at $\bar{p} > 3.5$ require that higher species (e.g., $ZnIm_5^{2+}$ and $ZnIm_6^{2+}$) be considered. A six-species model with reasonable formation constants for the fifth and sixth complexes provides satisfactory interpretation of all data. Implications of those observations with respect to biologically active zinc(II) proteins are considered.

I. Introduction

The imidazole structure is one of primary importance in biological systems where it occurs in the amino acid histidine and as part of the purine ring in nucleic acid structures. It has been implicated as the site of H-bond formation which influences protein conformation and can facilitate proton-transfer reactions.[2] It also appears to be the site of metal-ion complexation in many enzyme systems[2] and may be the site of interaction between certain antitumor agents and nucleic acids.[3-6]

In particular, a number of Zn(II) enzymes involve connections between zinc and two or more imidazole groups of histidine residues in the protein structure. Because of the lack of suitable magnetic or spectroscopic properties for the d^{10} Zn^{2+} ion, the interaction site is most often explored by substitution of another transition-metal ion, such as Ni^{2+}, Co^{2+}, and Cu^{2+}, which lend themselves more readily to analysis by modern spectrometric or magnetic methods. While such techniques undoubtedly give valuable information concerning the metal-ion site, the question remains as to the applicability of the derived structural information to the Zn^{2+} complex itself.

Previous NMR work on imidazole solutions has mainly employed proton NMR techniques to study self-association and other equilibria in nonaqueous solvents with no labile protons.[7-11] In a recent publication, Wasylishen and Tomlinson[12] have demonstrated a measurable dependence of ^{13}C shifts and ^{13}C–H coupling constants on pH in aqueous solutions of imidazole and L-histidine. Proton NMR studies of imidazole in aqueous solution suffer certain limitations due to rapid averaging of the imidazole NH proton with solvent protons. While such exchange may also influence the shape of the ^{15}N resonance in [^{15}N]imidazole, it generally does not preclude accurate measurement of the ^{15}N shift which is influenced by the changes in environment produced by the interactions of interest. Recent natural-abundance ^{15}N shift measurements in aqueous solutions of histidine as a function of pH demonstrate that protonation of the basic nitrogen of the imidazole ring produces a 30–50 ppm diamagnetic shift of its resonance.[13]

At intermediate pH values, complex formation constants for imidazole with Zn^{2+} indicate that significantly large concentrations of the various known complexes can be formed readily under reasonable conditions. Thus, chemical shifts occurring upon coordination may be investigated over a wide range of species distributions and at total imidazole concentrations sufficient to produce an easily measurable absorption signal with imidazole enriched in ^{15}N.

II. Experimental Section

^{15}N-Labeled imidazole was synthesized via the reaction

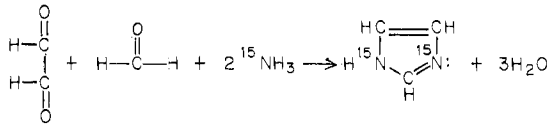

The method used was developed from the descriptions of Behrend and Schmitz.[14] A sketch of the reaction vessel is shown in Figure 1. Aqueous solutions of glyoxal (11.5 mL of Aldrich Chemical Co. 40% aqueous solution) and formaldehyde (7.6 mL of Mallinckrodt Analytical Reagent 37% aqueous solution) were combined in the 50-mL bulb which was then sealed off as indicated. The solution was cooled to 0 °C, with stirring, and the air was pumped out of the system. A total of 200 mmol of $^{15}NH_3$ (>98% ^{15}N) was then condensed via the vacuum-system manifold into the bottom of the 20 mm o.d. side arm by cooling it in liquid N_2. With the system isolated from the manifold, the side arm was allowed to come to room temperature, during which time the $^{15}NH_3$ first liquified (liquid occupied 5–6 mL of volume) and then was taken up (as it vaporized) by the continuously stirred glyoxal–formaldehyde solution. When the $^{15}NH_3$ uptake was complete, the reaction bulb was immersed in an oil bath to a depth such that the coarse frit was also immersed. With the side arm at room temperature, the reaction apparatus was continuously evacuated and the reaction mixture stirred while the oil bath temperature was slowly raised to a temperature of ~200 °C. The crude [^{15}N]imidazole distilled into the side arm at temperatures of 160–200 °C. It was a mixture of white crystals and yellow liquid and was purified by vacuum sublimation at 90–100 °C. After two or three such sublimations, the resulting pure [^{15}N]imidazole was a white crystalline solid melting at 89–90 °C. The yield was ~20% based upon the starting $^{15}NH_3$.

^{15}N NMR signals were obtained on a Varian XL-100 Fourier transform spectrometer operating at 10.158 MHz. The magnetic field was locked to the deuterium resonance in a sample of pure D_2O in a concentric capillary immersed in the working sample. The working sample was 2.0 mL of solution contained in a 12 mm o.d. spinning NMR tube. At a total imidazole concentration of 0.3 M, a peak with an S/N ratio of ~5:1 could be obtained in ~20 min of signal accumulation. ^{15}N shifts were measured relative to the deuterium lock frequency and also with respect to internal $(CH_3)_4{}^{15}N^+(NO_3^-)$. In all cases, the results agreed within the experimental uncertainty (±0.5

* To whom correspondence should be addressed at Los Alamos Scientific Laboratory.

0020-1669/78/1317-2288$01.00/0 © 1978 American Chemical Society

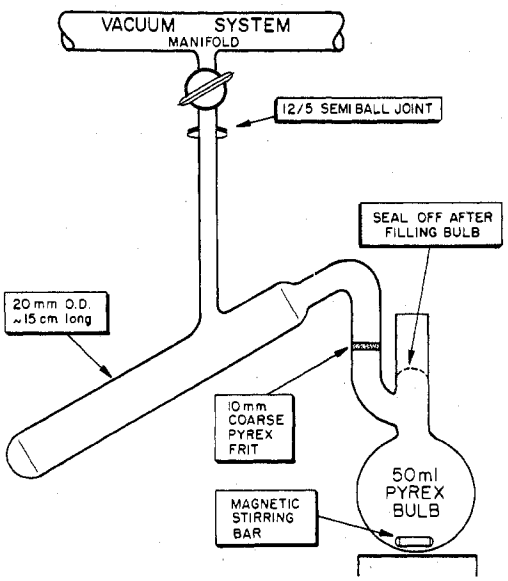

Figure 1.

ppm), indicating that susceptibility corrections were negligible over the range of compositions studied. All measurements were made at a temperature of 24.5 ± 0.5 °C.

Solutions of Zn(II) and [^{15}N]imidazole were prepared by mixing weighed amounts of [^{15}N]imidazole, distilled H_2O, standard dilute HNO_3 solution, and standard aqueous $Zn(NO_3)_2$ solution (prepared from Baker Analyzed Reagent $Zn(NO_3)_2 \cdot 6H_2O$; 0.0003% Cu, 0.0003% Fe). Since Cu^{2+} is known to complex imidazole quite strongly in aqueous solution,[15,16] it seemed advisable to determine experimentally the extent to which the Cu impurity in the $Zn(NO_3)_2 \cdot 6H_2O$ salt might contribute to the ^{15}N NMR parameters, especially the ^{15}N shift, in the zinc(II)–imidazole solutions. We accordingly prepared an aqueous solution (pH 5.9) which was 0.47 M in imidazolium ion and 0.03 M in neutral imidazole. Its ^{15}N spectrum was a multiplet with individual component widths of ~2 Hz and overall envelope width of ~15 Hz. To this solution we made appropriate stepwise additions of aqueous $Cu(NO_3)_2$, recording the ^{15}N spectrum after each addition, to cover a range of added Cu^{2+} concentrations of 10^{-6}–10^{-4} M. The significant finding was that a 10^{-6} M concentration of added Cu^{2+} was sufficient to collapse the ^{15}N multiplet structure to yield a singlet of ~15-Hz width at half-height with no measurable shift relative to the center of the original multiplet. When the added Cu^{2+} concentration reached 10^{-4} M, the ^{15}N resonance was a very broad singlet, ~200 Hz at half-height, but still unshifted relative to the center of the original multiplet. It thus seems clear that Cu^{2+} broadens so much more strongly than it shifts the ^{15}N resonance in aqueous imidazole that any signal which might be shifted significantly by Cu^{2+} would be difficult to detect due to extreme width. As the ^{15}N line width did not exceed 60 Hz in any of the zinc(II)–imidazole solutions used in this study, we conclude that, while Cu^{2+} impurities may contribute appreciably to the ^{15}N line width, they cannot make a significant contribution to the ^{15}N shift.

To maximize the signal-to-noise (S/N) ratio for a given total signal acquisition time using FT techniques, it is advantageous to know T_1 for the nucleus of interest under the conditions of the experiment. One may then obtain combinations of FT pulse widths and delay times (expressed as multiples of T_1) which yield the highest S/N for given total time spent in signal accumulation.[17] For this reason, ^{15}N T_1 measurements were made for [^{15}N]imidazole in aqueous solution under three general conditions: (1) At low pH (pH <5) where the imidazole was almost entirely in the form of the protonated imidazolium ion ($pK_a = 7.1$),[2a] T_1 for ^{15}N was 35 ± 5 s. (2) At pH >9 where imidazole exists as the aqueous base, one measures ^{15}N T_1 values of 15 s or less. (3) In solutions in which the imidazole was complexed by Zn^{2+} (mixture of species $ZnIm_i^{2+}$), T_1 was 6 ± 0.5 s. In cases (1) and (3) one observes large NOE effects on proton irradiation (large inverted signals) indicating predominantly dipolar relaxation via ^{15}N–proton coupling. Thus, the shorter relaxation times in the Zn^{2+} complexes are probably due to more favorable (longer) molecular reorientation times. In case (2) there were little, if any, NOE effects. However, if these solutions were treated with H_2S, T_1 values >1 min and large NOE effects were observed. These observations suggest strongly that in aqueous imidazole (at pH >9) T_1 is dominated by trace amounts of paramagnetic impurities for which the free base is a good complexing agent. We have not pursued the T_1 measurements in any detail since our only purpose here was to get an indication of their magnitudes as an aid in optimizing signal accumulation.

Table I. ^{15}N Chemical Shifts in Aqueous Imidazole Solutions (24.5 °C)

total [^{15}N]Im concn, M	mol fraction of [^{15}N]ImH$^+$, n	pH	^{15}N shift,[a] δ, ppm	δ/n, ppm
1.0	0.000	10.4	0 (ref)	
0.567[b]	0.000	9.6	0.0	
0.114[b]	0.000	10.1	0.0	
1.0	1.000	0.5	+31.0[c]	+31.0
0.599	1.000	1.90	+31.1	+31.1
0.571[b]	0.7475	6.61	+23.6	+31.6
0.618[b]	0.5082	7.08	+16.0	+31.5
0.584[b]	0.2628	7.54	+8.1	+30.8
1.0	0.000	13	−1	
1.0	0.000	14	−9.9	
			Av	+31.2 ± 0.3

[a] Uncertainty ±0.5 ppm, + sign = diamagnetic (upfield) shift. [b] Ionic strength maintained at 0.6 with $(CH_3)_4{}^{15}N^+$. [c] We determined the ^{15}N resonance in aqueous ImH$^+$ to be paramagnetically shifted by 130.7 ± 0.5 ppm relative to internal $(CH_3)_4{}^{15}N^+$. This is in good agreement with the value of 133 ± 12 ppm which may be derived from ^{14}N shift values for ImH$^+$ and $(CH_3)_4N^+$ reported by Herbison-Evans and Richards.[18]

Table II. ^{15}N Chemical Shifts in Aqueous Zinc(II)–Imidazole Solutions (24.5 °C)

sample no.	concn of total imidazole, [TL], M	total added HNO_3 concn, [TA], M	total Zn(II) concn, [TM], M	obsd ^{15}N shift,[a] ppm
I	0.2938	0.0569	0.2014	17.8
II	0.0884	0.0223	0.0223	17.3
III	0.1146	0.0197	0.0828	17.6
IV	0.0975	0.0252	0.00482	11.9
V	0.0966	0.0206	0.0311	18.2
VI	0.1012	0.0205	0.0513	17.8
VII	0.0895	0.0504	0.0100	22.8
VIII	0.1046	0.0493	0.00988	20.2
IX	0.0983	0.0590	0.0500	23.8
X	0.0989	0.0408	0.00826	18.4
XI	0.1009	0.03306	0.00658	14.9
XII	0.1043	0.0712	0.0516	25.5
XIII	0.3036	0.1480	0.00516	16.6

[a] Relative to uncomplexed aqueous [^{15}N]imidazole. All shifts are diamagnetic.

III. Results

Aqueous [^{15}N]Imidazole. ^{15}N shift data relevant to possible species in aqueous solutions of [^{15}N]imidazole are summarized in Table I. For all samples listed, a single resonance was observed for the imidazole species. In the strongly acidic samples (pH 0.5, 1.90) and strongly alkaline samples (pH 13, 14) the resonance was a multiplet due to ^{15}N coupling with the CH protons in the imidazole ring. (A detailed analysis and discussion of these multiplet structures will be presented in a separate publication.) For samples of intermediate pH, the resonance was a singlet of varying line width.

Zinc(II)–[^{15}N]Imidazole Solutions. ^{15}N shifts for [^{15}N]-imidazole in 13 solutions containing varying proportions of total Zn^{2+} to total imidazole were measured. Nitric acid was added to each solution to keep the pH below 9.0 to prevent precipitation of Zn^{2+} as the hydroxide.[15] In all cases, a single ^{15}N resonance was observed (with line width in the region of 18–60 Hz) indicating rapid averaging among all environments.

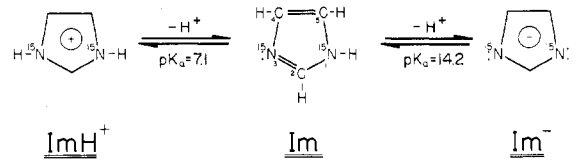

Figure 2.

The pertinent compositions and measured shifts are summarized in Table II. Without further resolution and interpretation those data do not reveal directly the desired information about contributions from individual species present in the equilibrium mixtures, although it is clear that Zn(II) species contribute sizable diamagnetic shifts to the overall averaged signal. As a result of the buffering capacity of Im in the applicable composition range, virtually all of the added acid appears as ImH^+, and the calculated shift attributable to that species in sample V, for example, is +6.7 ppm as compared to the observed 18.2 ppm upfield shift. Detailed species distributions are then required for assignment of the residual 11.5-ppm shift, as presented in the following section.

IV. Discussion

Aqueous [^{15}N]Imidazole. As previously indicated and shown in Figure 2, imidazole can take on a number of forms in aqueous solution depending upon pH.

For the species ImH^+ and Im^-, the two ^{15}N nuclei are equivalent and one expects only one ^{15}N resonance. For the species Im (for which the usual numbering system for the imidazole ring is indicated in Figure 2) in aqueous solution, the rapid exchange of the $^{15}N_1$ proton with H_2O protons has the effect of making $^{15}N_1$ and $^{15}N_3$ magnetically equivalent, and again only a single ^{15}N resonance is expected. However, as the average electronic environment in the vicinity of the nitrogen nuclei does change from one species to the next, a shift in the ^{15}N resonance with change in pH is expected. Moreover, since the neutral species, Im, has both a "pyridine-like" nitrogen with basic lone-pair electrons and a "pyrrole-like" nitrogen with a weakly acidic proton, it is capable of self-association by hydrogen bonding between neighboring Im molecules. This association has been studied[7,11] in nonaqueous media by observing the shift of the N_1 proton NMR signal as a function of total imidazole concentration. The proton resonance is a single peak representing rapid averaging of the proton between hydrogen-bonded and non-hydrogen-bonded species. It moves to lower field with increasing total imidazole concentration, which favors a higher degree of self-association. In aqueous solution such a study would be severely hampered by rapid exchange of the N_1 proton with solvent protons. However, in hydrogen bonds of the type ^{15}N···H–Y, previous studies with ammonia and the methylamines[19-21] have shown that the ^{15}N chemical shift can change by as much as 5–10 ppm when Y changes from O to N. Since any self-association of imidazole in aqueous solution results in such a change in the $^{15}N_3$ environment, it might be expected to produce an ^{15}N shift dependent upon total imidazole concentration.

The significant results displayed in Table I are the following: (a) The absence of any measurable ^{15}N shift over a 10-fold (0.1–1.0 M) change in total imidazole concentration suggests no significant self-association of imidazole via hydrogen bonding in aqueous solution. However, it is also possible that the results for the simple amines cited above are not applicable to imidazole and that the changes in hydrogen-bonding environment accompanying self-association of imidazole simply produce negligible ^{15}N shifts. What relevance the absence of ^{15}N shift might have with respect to self-association by other means, e.g., stacking with or without intervening solvent layers, is uncertain since we have no experience from which to infer what effect such association might have on the ^{15}N shift. We therefore can only conclude that the absence of ^{15}N shift as a function of total imidazole concentration provides no evidence for association of any kind but does not necessarily rule it out. (b) In the species ImH^+, the ^{15}N resonance is shifted diamagnetically (appears at lower frequency in a fixed magnetic field) by 31.2 ppm relative to the solvated Im species. That is consistent with the direction of the protonation shift for ^{14}N in pyridine[18] but is only about $^1/_2$ as great after correction for the averaging over the two nitrogens in imidazole. The protonation shift for imidazole is also comparable in direction and magnitude to the previously cited[13] protonation shift for the basic nitrogen of the imidazole ring of histidine. (c) At high pH, the ^{15}N resonance begins to shift paramagnetically because of the presence of Im^-, deprotonated at N_1. Roughly half of the total imidazole should be in the form of Im^- at pH 14, and since the average shift is ~10 ppm paramagnetically with respect to aqueous Im, it may be inferred that the ^{15}N shift for the Im^- species itself is ~20 ppm in the same direction. (d) In solutions with varying ratios of Im to ImH^+, the ^{15}N shift for the single averaged peak is a linear function of the mole fraction of ImH^+. This is demonstrated by the constancy of the ratio of observed shift to mole fraction of ImH^+ in samples at intermediate pH at a constant ionic strength of 0.6. The average ^{15}N shift per unit mole fraction of ImH^+, +31.2 ppm, may be used with shift and pH data to calculate pK_a for ImH^+: $pK_a = pH - \log([Im]/[ImH^+])$ or $pK_a = pH - \log(31.2/^{15}N\ shift) - 1$. For the three Im–$ImH^+$ mixtures, $pK_a = 7.09 \pm 0.01$ at 24.5 °C and $\mu = 0.6$. This is essentially the same as the reported $pK_a = 7.12$ at 25 °C and $\mu = 0.16$.[15,22] Thus, it appears that the equilibrium constant for ionization of ImH^+ is not strongly dependent upon ionic strength in this range.

Aqueous Zinc(II)–[^{15}N]Imidazole Solutions. Stepwise formation constants for complexes of Zn^{2+} and imidazole in dilute aqueous solution as determined by pH titration[15,16] and by the effect of Zn^{2+} on the hydrolysis of *p*-nitrophenyl acetate by Im,[16] have been reported. The highest complex required to interpret the work adequately, at 25 °C and $\mu = 0.16$, was $ZnIm_4^{2+}$. As Zn^{2+} is a diamagnetic species, large ^{15}N line broadening is not anticipated on complexation of [^{15}N]Im with Zn^{2+}. Thus, even a small shift in the ^{15}N resonance due to association of the nitrogen lone-pair electrons with Zn^{2+}, instead of H_2O protons, should be measurable. Moreover, if electrostatic effects are important, one might reasonably expect such shifts to be in the same direction as that produced by protonation of the lone pair (i.e., diamagnetic relative to aqueous Im).

As indicated earlier, the data in Table II demonstrate that complexation of imidazole by Zn^{2+} does in fact produce a measurable diamagnetic shift in the ^{15}N resonance of the imidazole nitrogen relative to uncomplexed aqueous imidazole. To treat these data in more quantitative fashion, we first solve the following set of equations for each of the 13 experimental solutions, where [L] = equilibrium concentration of free aqueous ligand (Im), [M] = equilibrium concentration of uncomplexed aqueous Zn^{2+}, $[ML_i]$ = equilibrium concentration of $ZnIm_i^{2+}$ complex, [LH] = equilibrium concentration of ImH^+, [H] = equilibrium concentration of hydrogen ion, [TL] = total concentration of ligand in all forms, [TM] = total concentration of zinc in all forms, [TA] = total concentration of added HNO_3, and K_w = ion product for $H_2O = 1 \times 10^{-14}$. (While 1×10^{-14} may not be the precise value for K_w at $\mu = 0.6$, under the present experimental conditions the term involving K_w makes a negligible contribution to [TA] as long as $pK_w \geq 11$.)

$$K_i = \frac{[ML_i]}{[ML_{i-1}][L]}$$

$$K_A = \frac{[L][H]}{[LH]} = 10^{-7.09}$$

$$[TM] = [M] + \sum_i [ML_i]$$

$$[TL] = [L] + [LH] + \sum_i i[ML_i]$$

$$[TA] = [H] + [LH] - \frac{K_w}{[H]}$$

Given values for the compositional parameters [TM], [TL], and [TA] (listed in Table II), only values for the K_i are required to solve the above system of $i + 4$ equations for the $i + 4$ species concentrations, $[ML_1]$, $[ML_2]$, ..., $[ML_i]$, [L], [M], [LH], and [H]. These derived concentrations may then be used in conjunction with the measured ^{15}N shifts (listed in Table II) to examine in detail the ^{15}N shift resulting from complexation of [^{15}N]imidazole by Zn^{2+}. We were especially interested in testing the possibility that the average shift for an imidazole in the complex $ZnIm_i^{2+}$ might vary with i. We have used two general approaches in making this test. In the first approach, we calculated for each solution the average ^{15}N shift for all the complexed imidazole. This is given by $\bar{\delta} = (\delta_{obsd} - f_{LH} \times 31.2)/\sum_i f_i$, where $f_{LH} = [LH]/[TL]$ and $f_i = i[ML_i]/[TL]$. This "average ^{15}N shift for a bound imidazole" is then plotted against the average number of imidazoles bound by a given Zn^{2+}, $\bar{\nu} = ([TL] - [L] - [LH])/[TM]$. Any variation of $\bar{\delta}$ with $\bar{\nu}$ is indicative of a dependence of ^{15}N shift on i in the species $ZnIm_i^{2+}$. Figure 3 is a plot of $\bar{\delta}$ vs. $\bar{\nu}$ resulting from a treatment of the data according to the scheme just outlined, *assuming* a maximum of four $ZnIm_i^{2+}$ species and using the K_i values reported by Koltun et al.,[16] viz., $K_1 = 4 \times 10^{1.92}$, $K_2 = {}^3/_2 \times 10^{2.14}$, $K_3 = {}^2/_3 \times 10^{2.50}$, and $K_4 = {}^1/_4 \times 10^{2.65}$.[31]

This plot demonstrates three important points: (a) that complexation of imidazole by Zn^{2+} results in large diamagnetic ^{15}N shifts relative to aqueous uncomplexed imidazole; (b) the average ^{15}N shift for a bound imidazole appears to increase significantly with the average coordination number of Zn^{2+}; and (c) there is a rather abrupt change in trend at $\bar{\nu} > 3.53$.

A second, more detailed treatment of the data can, at least in principle, yield the average ^{15}N shift for the imidazole in each $ZnIm_i^{2+}$ complex, assuming rapid averaging among all species. Thus, for a given solution the observed ^{15}N shift is given by

$$\delta_{obsd} = f_{LH}\delta_{LH}^{\circ} + f_1\delta_1^{\circ} + f_2\delta_2^{\circ} + f_3\delta_3^{\circ} + f_4\delta_4^{\circ} \qquad (A)$$

where f_{LH} = fraction of total imidazole as ImH^+, δ_{LH}° = ^{15}N shift for ImH^+ relative to aqueous Im = 31.2 ppm, f_i (i = 1–4) = fraction of total imidazole as species $ZnIm_i^{2+}$, and δ_i° = average ^{15}N shift for imidazole in species $ZnIm_i^{2+}$ relative to aqueous Im. An indicated earlier, all species concentrations (hence all the f_i in the above equation) can be calculated given the compositional parameters (listed in Table II) and values for K_i ($ZnIm_i^{2+}$ complexation constants). By assuming the K_i values of Koltun et al.,[16] the 13 experiments could then provide 13 equations in four unknowns from which the δ_i° which best fit all 13 equations could be derived. However, since the above authors did not exceed $\bar{\nu} > 3.14$ in their determination of the K_i and since our plot of $\bar{\delta}$ vs. $\bar{\nu}$ (Figure 3) shows a significant change in trend at $\bar{\nu} > 3.53$, we derived best values of δ_i° from a least-squares fit of the data for the nine experiments in which $\bar{\nu} \leq 3.53$. The results are $\delta_1^{\circ} = 10.9 \pm 1.3$, $\delta_2^{\circ} = 16.8 \pm 3.8$, $\delta_3^{\circ} = 16.0 \pm 3.5$, and $\delta_4^{\circ} = 16.5 \pm 1.7$, all in ppm and diamagnetically shifted relative to aqueous Im. The uncertainties are standard deviations resulting from the best computer fit. The solid curve in Figure 3 is based upon assuming the above δ_i° values to calculate $\bar{\delta}$ for each solution using equation A. The fit to the experimental points is well within the experimental uncertainty except at $\bar{\nu} > 3.53$. Moreover, the derived values of δ_i° do not seem unreasonable. The previous[15,16] work demonstrates that the *intrinsic* association constants for complexation of Zn^{2+} by imidazole increase progressively with increasing coordination number ($\kappa_1 = 83.2$, $\kappa_2 = 138.0$, $\kappa_3 = 316.2$, $\kappa_4 = 446.7$). This indicates a stronger average interaction between Zn^{2+} and imidazole with increasing coordination number. Since the interaction between Zn^{2+} and imidazole almost certainly involves the $^{15}N_3$ lone-pair electrons, this stronger average interaction might be expected to lead to greater perturbation of the electron density in the vicinity of the ^{15}N nucleus and, therefore, lead to an increase in δ_i° with increasing coordination number. Since the uncertainties in the derived δ_i° values are large, a trend to higher values with increasing i is not inconsistent with the results. It is also interesting to compare the ^{15}N shift produced on complexation with Zn^{2+} to that produced by protonation of Im to form ImH^+. In both cases, a diamagnetic shift is produced but the magnitude of the shift produced by protonation (31.2 ppm) is roughly 2–3 times as great as that produced by Zn^{2+} complexation. If one assumes a primarily electrostatic interaction between the $^{15}N_3$ lone pair and a diamagnetic positive ion, it seems reasonable to expect that both interactions would shift the ^{15}N resonance in the same direction with the stronger interaction (protonation) producing the larger shift.

Although the ^{15}N shift data at $\bar{\nu} \leq 3.53$ are consistent with a maximum coordination number of 4 for zinc(II)–imidazole complexes, the data at $\bar{\nu} > 3.53$ are clearly inconsistent with

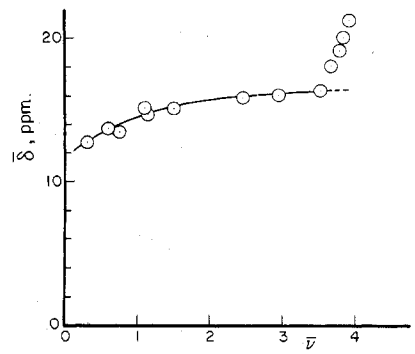

Figure 3. ^{15}N shifts in $ZnIm_i^{2+}$ complexes ($1 \leq i \leq 4$).

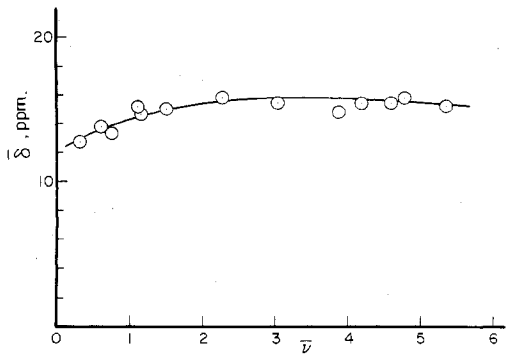

Figure 4. ^{15}N shifts in $ZnIm_i^{2+}$ complexes ($1 \leq i \leq 6$).

Table III

$K_1 = 6 \times 10^{1.74}$	$\delta_1^{\circ} = 11.5$	$K_4 = {}^3/_4 \times 10^{2.17}$	$\delta_4^{\circ} = 16.0$
$K_2 = {}^5/_2 \times 10^{1.92}$	$\delta_2^{\circ} = 15.5$	$K_5 = {}^2/_5 \times 10^{1.90}$	$\delta_5^{\circ} = 15.5$
$K_3 = {}^4/_3 \times 10^{2.20}$	$\delta_3^{\circ} = 16.0$	$K_6 = {}^1/_6 \times 10^{1.75}$	$\delta_6^{\circ} = 15.2$

this model. We believe that this constitutes evidence for formation at higher $\bar{\nu}$ of $ZnIm_i^{2+}$ species with $i > 4$. Though we are unaware of any previous evidence for such species in solution, the species $ZnIm_6^{2+}$, for example, has been clearly identified in crystalline solids.[23,24] We, therefore, felt it would be worthwhile to attempt a fit of all our ^{15}N shift data utilizing a six-species model which retains the same association constants reported by Koltun et al.[16] for the first four complexes and assumes "reasonable" association constants for formation of $ZnIm_5^{2+}$ and $ZnIm_6^{2+}$. By a process of trial and error, using the same calculational techniques employed for the four-species treatment, the fit shown in Figure 4 was obtained. The corresponding K_i and $\delta_i°$ values are listed in Table III. It should be noted that the values of K_1 through K_4 are identical with those reported by Koltun et al.[16] but are expressed in terms of statistical factors (pre-exponential terms) consistent with six rather than four coordination sites. The resulting "intrinsic" association constants, κ (the exponential term in each case), are, therefore, different from those reported by the above authors. They display a similar trend of increasing κ with increasing coordination number except between $\kappa_3 = 10^{2.20}$ and $\kappa_4 = 10^{2.17}$ where a reversal of this trend appears in the six-coordinate relative to the four-coordinate treatment. We therefore assumed a continuing trend to lower values for κ_5 and κ_6. The values of $\log \kappa_5 = 1.90$ and $\log \kappa_6 = 1.75$ lead to the least scatter in the plot of $\bar{\delta}$ vs. $\bar{\nu}$ in Figure 4. (Changes of ± 0.1 in these values lead to significantly greater scatter.) The solid curve in Figure 4 is derived from the $\delta_i°$ values listed in Table III. These were determined by trial and error to give the best fit to the plotted points. The first four values are essentially equal to those derived from the four-species fit at lower $\bar{\nu}$ values. We conclude that a six-species model with reasonable K_i and $\delta_i°$ values provides an adequate interpretation of all the experimental data. Attempts to fit the data with a maximum of five species leads to a significantly poorer fit. Moreover, if the six-parameter model with the K_i listed in Table III is used with the solution composition parameters of Koltun et al.,[16] the pH of each of their solutions may be calculated and compared with their measured pH. In every case, the discrepancy is ≤ 0.02 pH unit which indicates that the fifth and sixth species would not have contributed significantly to their experimental observations.

V. Concluding Remarks

The variation of intrinsic formation constants reported here is consistent with the concept that π-acceptor properties of imidazole lead to enhanced stability of O donors in mixed-ligand complexes.[2a,25] That appears in this case as a decrease in intrinsic formation constants for the fourth, fifth, and sixth species. These data indicate that the coordination numbers of mixed imidazole–water complexes of Zn(II) are probably six across the entire range of possible species. If it is indeed true that "much of the specificity and many of the properties so far only associated with metal-ion complexation in macromolecular biological systems are inherent already in relatively simple coordination compounds"[25] and that "catalysis by metalloenzymes may be a reflection of the chemistry of the metal ion itself as a Lewis acid",[26] then consideration of the role of Zn(II), with ligands such as histidine (imidazole) and water, in zinc proteins should probably be based on octahedral geometry. Deviations from such structures may then be correlated with observed activities involving the metal-ion centers, so that it is perhaps more proper to speak of "defect octahedral" rather than "distorted tetrahedral" coordination environments for Zn(II), even when four-coordination is observed for a given state of the macromolecule.

Rosenberg et al.[27] found the coordination geometry in solutions of nickel(II) carboxypeptidase A to be "octahedral-like", while that of the Co(II) enzyme was said to be, less firmly, five-coordinate, with undefined structure, in evaporated films of the solid. The crystalline Zn(II) enzyme has been reported to be four-coordinate, with two histidine, one glutamic acid, and one water ligand, from the three-dimensional structure determination.[28] We suggest that the apparent structural differences among the comparably active Ni(II), Co(II), and Zn(II) enzymes may not so much involve flexibility of the coordination site with respect to protein ligands as it does variation in relative affinities for ions or small molecules, such as H_2O, having activities reflecting the specific conditions in the region of the metal-ion site required for a given observation. Such a system is not inherently "thermodynamically strained" but should be quite reactive toward other potential ligands which may become available with a change in conditions. Thus, the requirements for crystallization of a metalloenzyme may well dictate the number and configuration of small molecules coordinated to the metal ion, without necessarily affecting, significantly, the coordination geometry of the protein side-chain ligands.

A situation more nearly characteristic of aqueous solution behavior is found in the hexamer of zinc insulin, which contains two structurally significant Zn(II) atoms.[29] In that case, the metal atoms are reported to be at trigonal sites and each is thought to be coordinated to three histidine ligands (from three separate insulin dimers) and three H_2O molecules,[30] producing essentially octahedral structures as expected on the basis of a $[Zn(Im)_3(H_2O)_3]^{2+}$ aqueous solution model.

The majority of ^{15}N magnetic resonance spectra obtained in this work were for solutions having concentrations of the order of 0.1 M imidazole. Maximum reasonable aqueous solution concentrations for a protein with a molecular weight of $\sim 50\,000$ are of the order of 2×10^{-3} M. Incorporation of 100 atom % [^{15}N]histidine would permit shift measurements to be made on proteins of that molecular weight, if the spectrometer sensitivity were 50 times greater than that of the equipment used for this work. A current "state of the art", high-frequency, large-bore spectrometer should have that capability and allow direct observation of histidine coordination to Zn(II) in the protein.

Acknowledgment. This work was performed under the auspices of the U.S. Department of Energy.

Registry No. $ZnIm_4(H_2O)_2^{2+}$, 66610-68-2.

References and Notes

(1) (a) Los Alamos Scientific Laboratory. (b) University of Texas.
(2) (a) R. J. Sundberg and R. B. Martin, *Chem. Rev.*, **74**, 471 (1974); (b) C. A. Matuszak and A. J. Matuszak, *J. Chem. Educ.*, **53**, 280 (1976).
(3) P.-C. Kong and T. Theophanides, *Inorg. Chem.*, **13**, 1167 (1974).
(4) L. L. Munchausen, *Proc. Natl. Acad. Sci. U.S.A.*, **71**, 4519 (1974).
(5) I. A. G. Roos, A. J. Thompson, and S. Mansy, *J. Am. Chem. Soc.*, **96**, 6484 (1974).
(6) S. Mansy, B. Rosenberg, and A. J. Thompson, *J. Am. Chem. Soc.*, **95**, 1663 (1973).
(7) N. Joop and H. Zimmermann, *Ber. Bunsenges. Phys. Chem.*, **66**, 541 (1962).
(8) S. M. Wang and N. C. Li, *J. Am. Chem. Soc.*, **88**, 4592 (1966).
(9) H. M. Fales, E. Sokolski, and C. J. Martin, *Bioorg. Chem.*, **2**, 235 (1973).
(10) B. S. Tovrog and R. S. Drago, *J. Am. Chem. Soc.*, **96**, 2743 (1974).
(11) D. J. Doonan and A. L. Balch, *J. Am. Chem. Soc.*, **97**, 1403 (1975).
(12) R. E. Wasylishen and G. Tomlinson, *Biochem. J.*, **145**, 605 (1975).
(13) K. Kawano and Y. Kyogoku, *Chem. Lett.*, 1305 (1975).
(14) R. Behrend and J. Schmitz, *Justus Liebigs Ann. Chem.*, **277**, 310 (1893).
(15) J. T. Edsall, G. Felsenfeld, D. S. Goodman, and F. R. N. Gurd, *J. Am. Chem. Soc.*, **76**, 3054 (1954).
(16) W. L. Koltun, R. N. Dexter, R. E. Clark, and F. R. N. Gurd, *J. Am. Chem. Soc.*, **80**, 4188 (1958).
(17) K. A. Christensen, D. M. Grant, E. M. Schulman, and C. Walling, *J. Phys. Chem.*, **78**, 1971 (1974).
(18) D. Herbison-Evans and R. E. Richards, *Mol. Phys.*, **8**, 19 (1964).
(19) W. M. Litchman, M. Alei, Jr., and A. E. Florin, *J. Am. Chem. Soc.*, **91**, 6574 (1969).
(20) M. Alei, Jr., A. E. Florin, and W. M. Litchman, *J. Am. Chem. Soc.*, **92**, 4828 (1970).
(21) M. Alei, Jr., A. E. Florin, W. M. Litchman, and J. F. O'Brien, *J. Phys. Chem.*, **75**, 932 (1971).
(22) C. Tanford and M. L. Wagner, *J. Am. Chem. Soc.*, **75**, 434 (1953).

(23) C. Sandmark and C. Brändén, *Acta Chem. Scand.*, **21**, 993 (1967).
(24) D. M. L. Goodgame, M. Goodgame, P. J. Hayward, and G. W. Rayner-Canham, *Inorg. Chem.*, **7**, 2447 (1968).
(25) H. Sigel, B. E. Fischer, and B. Prijs, *J. Am. Chem. Soc.*, **99**, 4489 (1977).
(26) N. E. Dixon, C. Gazzola, R. L. Blakley, and B. Zerner, *Science*, **191**, 1144 (1976).
(27) R. C. Rosenberg, C. A. Root, and H. B. Gray, *J. Am. Chem. Soc.*, **97**, 21 (1975).
(28) F. A. Quiocho and W. N. Lipscomb, *Adv. Protein Chem.*, **25**, 1 (1971); W. N. Lipscomb, *Chem. Soc. Rev.*, **1**, 319 (1972).
(29) A. S. Brill and J. H. Venable, *J. Am. Chem. Soc.*, **89**, 3622 (1968).
(30) T. Blundell, G. Dodson, D. Hodgekin, and D. Mercola, *Adv. Protein Chem.*, **26**, 279 (1972).
(31) The overall stepwise formation constants are expressed here as the product of two terms; a "statistical" term and an "intrinsic" formation constant expressed in exponential form. The statistical factor depends upon the assumed number of equivalent coordination sites available to the incoming ligand. Thus, in the equilibrium $ML_i + L \rightleftarrows ML_{i+1}$ if M has four equivalent coordination sites there are $4 - i$ sites available to an incoming ligand and $i + 1$ sites from which a ligand can dissociate. Thus, the formation of ML_{i+1} is biased by a purely probabilistic or "statistical" factor of $(4 - i)/(i + 1)$. If one assumes six equivalent coordination sites the statistical factor is $(6 - i)/(i + 1)$. Dividing the overall formation constant by the statistical factor yields the so-called "intrinsic" formation constant which is a measure of the binding strength for a single coordination site in the species ML_i. For a more detailed description of this kind of treatment see ref 32.
(32) A. R. Burkin, *Q. Rev., Chem. Soc.*, **5**, 1 (1951).

Contribution from Ames Laboratory—U.S. Department of Energy, Iowa State University, Ames, Iowa 50011

Synthesis and Characterization of New Metal–Metal Bonded Species. 3. Dimeric Tantalum(III) Halide Adducts with Tetrahydrothiophene. Characterization of Structure-Bonding Features through NQR Spectroscopy

J. L. TEMPLETON and R. E. McCARLEY*

Received December 29, 1977

The synthesis of the first tantalum(III) halide adducts $Ta_2X_6(SC_4H_8)_3$ (X = Cl, Br) is described. Properties of these diamagnetic dimers are related to the known metal–metal bonded confacial bioctahedral structure which consists of two halogen atoms and the sulfur of one tetrahydrothiophene ligand bridging between the two metal atoms with two halogen atoms plus one tetrahydrothiophene bound as terminal ligands on each metal. The ^1H NMR, infrared, and UV–visible spectra all correlate well with the important structural features. NQR spectra are reported for the halogen nuclei as well as for ^{93}Nb in the homologous series of crystalline derivatives $Nb_2X_6(SC_4H_8)_3$ (X = Cl, Br, I) and $Ta_2X_6(SC_4H_8)_3$ (X = Cl, Br). In the structurally characterized bromides the ^{81}Br spectra correlate fully with the known unit cell symmetry; in these cases four resonances at lower frequency and two at higher frequency are definitively assigned to the terminal and bridging bromine atoms of the dimer, respectively. Strong π back-bonding from halogen to metal results in lower resonance frequencies for the terminal halogen atoms as compared to the frequencies of the bridging atoms in all cases. The ^{93}Nb NQR coupling constants of the three niobium dimers increase in the order Cl < Br < I. This order is consistent with a nearly constant contribution from d electrons involved in metal–metal bonding to the niobium NQR and decreasing contribution from d electrons involved in metal–ligand bonding to the net ^{93}Nb electric field gradient.

Introduction

There are still broad gaps in our knowledge concerning chemistry of the lower oxidation state halide complexes of niobium and tantalum.[1] In particular, there is an absence of information regarding well-characterized tantalum(III) halide complexes. The trihalides of tantalum are nonstoichiometric exhibiting compositions from $TaX_{2.9}$ to $TaX_{3.1}$.[2] The insolubility and lack of reactivity which characterize the trihalides make them unacceptable for synthetic manipulations directed toward derivatives of tantalum(III).

The descriptive chemistry of tantalum is dominated by the pentavalent complexes which constitute the majority of compounds reported to date.[3] The tetrahalides of tantalum are well characterized, and quadrivalent derivatives have been examined in recent years.[4] No trivalent halide complexes of tantalum have been confirmed in the literature. Blight, Deutscher, and Kepert reported that the reaction of $TaCl_4$ and acetonitrile led to the formation of $[TaCl_3(CH_3CN)_2]_2$,[5] which formally appears to correspond to tantalum(III). More recently McCarley and co-workers communicated the crystal structure of $\{[(C_6H_5)_3P]_2N\}_2\{Nb_2Cl_8(CH_3CN)_2C_4H_6N_2\}$ after a thorough investigation of the chemistry of niobium and tantalum tetrahalides in acetonitrile led to the above salt in order to elucidate the redox chemistry involved in these systems.[6] The culmination of the investigation was the identification of a unique bridging ligand revealed by the structure which resulted from the reductive coupling of two acetonitrile molecules and was accompanied by oxidation of the niobium to the 5+ oxidation state. It seems probable that the dimeric species isolated from earlier tantalum tetrachloride reactions with acetonitrile is a similar ligand-bridged complex of tantalum(V).

Previous work in this laboratory provided the new compounds of niobium(III) $Nb_2X_6(SC_4H_8)_3$ with X = Cl, Br, or I.[7] Since niobium is more easily reduced than tantalum and discrete halide complexes of tantalum(III) were unknown, the synthesis and characterization of molecular tantalum halide adducts of the form $Ta_2X_6(SC_4H_8)_3$ with X = Cl or Br were undertaken. In this report are described the synthetic route which led to isolation of the first tantalum(III) halide adduct with tetrahydrothiophene and the physical studies of these complexes. The complete crystal and molecular structure analysis of $Nb_2Br_6(SC_4H_8)_2$ and $Ta_2Br_6(SC_4H_8)_3$ reported previously[8] has shown that the compounds exist as molecular dimers with a confacial octahedral configuration[9] whereby the metal atoms are bridged by two bromine atoms and the sulfur atom of one tetrahydrothiophene ligand.

Experimental Section

The tantalum halides of interest in this study were all air and moisture sensitive. Manipulations of solids were therefore performed in a nitrogen-filled drybox and standard vacuum line techniques were employed for solvent transfers. Tantalum pentahalides were prepared

0020-1669/78/1317-2293$01.00/0 © 1978 American Chemical Society